A New Reduced-Order Model of SAW Interdigital Transducers

Oscar Antonio Peverini, Renato Orta, *Senior Member, IEEE*, and Riccardo Tascone

***Abstract*—The Green's function method is generally agreed to be the most satisfactory technique for the rigorous analysis of surface-acoustic-wave interdigital transducers (IDTs). However, its direct application to response investigations or optimization-based design activities is limited by its computational complexity. In this paper, we present a new reduced-order model of IDTs based on a moment-matching technique and on the singular value decomposition. Several numerical and experimental examples demonstrate the accuracy and the efficiency of the method.**

***Index Terms*—Cauchy method, interdigital transducers, reduced-order model, SAW devices.**

I. Introduction

In RECENT years, advances in both theory and computation have allowed to develop computer-aided design (CAD) software based on the Green's function method (GFM) for the rigorous analysis of surface-acoustic-wave (SAW) devices [1], [2]. As is well known, the analysis via the GFM requires the solution of a linear system of size $N \times N$, where N is the number of basis functions used to represent the unknown charge distribution. The two major factors affecting the GFM computational efficiency are the evaluation of the moment matrix and the solution of the linear system. Although an efficient implementation of the GFM can take advantage from a suitable choice of the basis function set [3] and from the use of iterative algorithms, as the general minimization of residues (GMRES) [4], the computational complexity of the method may be still too high for the direct application in optimization-based design activities and in the analysis of long and nonperiodic structures.

Recently, model order-reduction techniques based on moment matching and the Padé approximation, such as the method of asymptotic waveform evaluation (AWE) and the Cauchy method, were applied with success to the analysis of several electromagnetic devices [5], [6]. The basic idea of these methods is to develop an approximate transfer function of a given linear system from a limited set of spectral solutions and of its derivatives (moments). In this paper, for the first time, the Cauchy method has been applied to the frequency-response evaluation of SAW interdigital transducers (IDTs). In order to increase the computational efficiency of the method, a new set of orthogonalized problem-matched basis functions, numerically generated via singular value decomposition (SVD), are used to expand the unknown charge density and almost analytical expressions for the moments have been derived. The authors demonstrate the accuracy and the advantages of the proposed method for several transducer configurations. The present technique allows a reduction of the CPU time of about one order of magnitude in comparison with the direct application of the GFM in conjunction with the GMRES algorithm without any significant loss of accuracy.

Manuscript received July 28, 2000; revised January 31, 2001.

O. A. Peverini and R. Orta are with the Department of Electronics, Politecnico di Torino, 10129 Turin, Italy (e-mail: peverini@athena.polito.it; orta@polito.it).

R. Tascone is with the Istituto di Ricerca sull'Ingeneria delle Telecomunicazioni e dell'Informazione, Consiglio Nazionale delle Ricerche, 10129 Turin, Italy (e-mail: tascone@athena.polito.it).

Publisher Item Identifier S 0018-9480(01)08693-8.

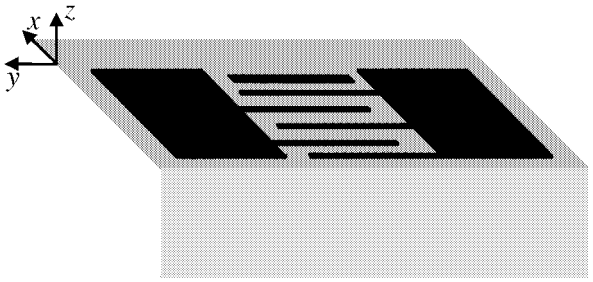

Fig. 1. Geometry of the IDT.

II. GFM

The type of IDTs analyzed here consists of an array of electrodes parallel to the y-axis, printed on the surface $z = 0$ of a piezoelectric substrate, as shown in Fig. 1. In a two-dimensional analysis, in which the mass-loading effect is neglected, the potential $\Phi(x)$ on the surface $z = 0$ is related to the surface charge density $\sigma(x)$ by the convolution integral

$$\Phi(x) = \int_{-\infty}^{+\infty} G(x - x')\sigma(x')\,\mathrm{d}x' \tag{1}$$

where $G(x)$ is the electric Green's function of the substrate. Also, the analysis of apodized IDTs can be performed in this framework by introducing the concept of equivalent voltage apodization, in which, however, diffraction effects are ignored [7]. The IDT behavior is described by the integral equation

$$\sum_{i=1}^{M} V_i \mathrm{P}_{W_i}(x) = \int_{-\infty}^{+\infty} G(x - x')\sigma(x')\,\mathrm{d}x' \qquad \forall x \in W_\mathrm{t} \tag{2}$$

where i labels the various fingers and $W_\mathrm{t} = \cup_{i=1}^{M} W_i$ denotes the union of the M fingers of the transducer. $\mathrm{P}_{W_i}(x)$ is a pulse function with support W_i and V_i is the relevant applied voltage. In order to solve the integral equation (2) by means of

the Galerkin's method of moments, we introduce a set of basis functions $\{f_n(x)\}$ and expand $\sigma(x)$ as

$$\sigma(x) = \sum_{n=1}^{N} \alpha_n f_n(x) \tag{3}$$

where α_n are unknown charge coefficients and N is the number of basis function defined on the whole transducer. Substituting (3) into (2) and projecting upon the set of basis functions yields

$$\Phi_m = \sum_{n=1}^{N} L_{mn}\alpha_n, \qquad m = 1, \ldots, N \tag{4}$$

where

$$\Phi_m = \sum_{i=1}^{M} V_i \int f_m^*(x)\mathrm{P}_{W_i}(x)\,\mathrm{d}x \tag{5}$$

$$L_{mn} = \iint f_m^*(x)G(x-x')f_n(x')\,\mathrm{d}x'\,\mathrm{d}x. \tag{6}$$

With slight modifications, this formulation can be applied to the IDT with loaded, shorted, or isolated electrodes [8]. After solving the linear system of equations (4), we can compute the charge distribution and, from that, the IDT input admittance.

The Green's function $G(x)$ can be cheaply evaluated in the spectral domain ξ, where ξ is the spectral variable conjugate to x. The substrate backsurface is generally processed in order to reduce the coherence of reflected bulk waves so that the substrate is modeled here as semiinfinite. Hence, it is convenient to introduce the frequency-independent transformed Green's function $\Gamma(s) = \omega\tilde{G}(\xi/\omega)$, where $s = \xi/\omega$ is the slowness [9]. The function $\Gamma(s)$ may be decomposed as [3]

$$\Gamma(s) = \Gamma^{(\mathrm{el})}(s) + \Gamma^{(\mathrm{saw})}(s) + \Gamma^{(\mathrm{bulk,\,asy})}(s) + \Gamma^{(\mathrm{bulk,\,res})}(s) \tag{7}$$

where $\Gamma^{(\mathrm{el})}(s)$ is the electrostatic part, $\Gamma^{(\mathrm{saw})}(s)$ is the SAW contribution, $\Gamma^{(\mathrm{bulk,\,asy})}(s)$ is the extracted asymptotic bulk contribution, and $\Gamma^{(\mathrm{bulk,\,res})}(s)$ is the residual bulk part. All the contributions, except $\Gamma^{(\mathrm{bulk,\,res})}(s)$ for general case analysis, have analytical expressions [3].

Although weighted first-kind Chebyshev polynomials better suit the singularity of the charge distribution at the finger edges, in this paper, we use a set of pulse functions with different supports, which yield almost analytical expressions for the moments $L_{mn}^{(k)}$ (kth derivative of L_{mn} with respect to the angular frequency ω). These moments are required in the application of the Cauchy method to the approximation of the IDT transfer function, as explained in Section III. Therefore, we introduce the basis functions

$$f_n(x) = \frac{\mathrm{P}_{W_n}(x)}{2\epsilon_n}, \qquad n = 1, \ldots, N \tag{8}$$

with $W_n = [\delta_n - \epsilon_n,\ \delta_n + \epsilon_n]$, where δ_n and ϵ_n denote the midpoint coordinate and the half-width of the nth pulse. To maximize the representation efficiency of pulse functions, we can reduce their support as the finger edge is approached, so as to fit the divergent charge distribution. Since the Green's function is computed directly in the spectral domain, it is convenient to evaluate the L_{mn} matrix elements in the same domain by applying the Parseval's theorem. According to (7) and with the choice (8), the moments $L_{mn}^{(k)}$ can be decomposed as

$$L_{mn}^{(k)} = L_{mn}^{(\mathrm{el})^{(k)}} + L_{mn}^{(\mathrm{saw})^{(k)}} + L_{mn}^{(\mathrm{bulk,\,asy})^{(k)}} + L_{mn}^{(\mathrm{bulk,\,res})^{(k)}} \tag{9}$$

where we have distinguished the various contributions, as in (7). Obviously, the electrostatic term $L_{mn}^{(\mathrm{el})}$ does not depend on ω [10], so that the moments $L_{mn}^{(\mathrm{el})^{(k)}}$ vanish for $k \geq 1$. As for the moments $L_{mn}^{(\mathrm{saw})^{(k)}}$, it is possible to derive the following expressions for $k \geq 0$:

$$L_{mn}^{(\mathrm{saw})^{(k)}} = \frac{\jmath G_{\mathrm{saw}}}{4\epsilon_m\epsilon_n s_{\mathrm{saw}}^2\omega^{k+2}} \sum_{i=1}^{4} (-1)^{(i-1)}\mathrm{R}_k(X_i)\,\mathrm{e}^{-\jmath X_i} \tag{10}$$

for $m \neq n$ and

$$L_{nn}^{(\mathrm{saw})^{(k)}} = \frac{2G_{\mathrm{saw}}}{X_0}\left(\frac{2\epsilon_n s_{\mathrm{saw}}}{X_0}\right)^k \left(\beta_k + \frac{\jmath\gamma_k}{X_0} + \frac{\jmath \mathrm{S}_k(X_0)\,\mathrm{e}^{-\jmath X_0}}{X_0}\right) \tag{11}$$

for the diagonal terms; s_{saw} is the SAW slowness, G_{saw} is the residue of $\Gamma(s)$ at $s = s_{\mathrm{saw}}$, and

$$\begin{aligned} X_0 &= 2\omega s_{\mathrm{saw}}\epsilon_n \\ X_1 &= \omega s_{\mathrm{saw}}\big(|\delta_m - \delta_n| - \epsilon_n - \epsilon_m\big) \\ X_2 &= \omega s_{\mathrm{saw}}\big(|\delta_m - \delta_n| - \epsilon_n + \epsilon_m\big) \\ X_3 &= \omega s_{\mathrm{saw}}\big(|\delta_m - \delta_n| + \epsilon_n + \epsilon_m\big) \\ X_4 &= \omega s_{\mathrm{saw}}\big(|\delta_m - \delta_n| + \epsilon_n - \epsilon_m\big). \end{aligned} \tag{12}$$

Furthermore,

$$\mathrm{R}_0(X_i) = 1 \qquad \forall X_i \quad \mathrm{S}_0(X_0) = 1 \quad \forall X_0 \quad \beta_0 = \gamma_0 = -1. \tag{13}$$

For $k \geq 1$, the kth degree polynomials R_k and S_k and the coefficients β_k and γ_k can be derived by analytical differentiating (10) and (11).

As for the asymptotic bulk contribution $L_{mn}^{(\mathrm{bulk,\,asy})^{(0)}}$, it is possible to derive the following analytical expression:

$$L_{mn}^{(\mathrm{bulk,\,asy})^{(0)}} = \frac{C_\infty}{8\pi\epsilon_m\epsilon_n s_{\max}^2\omega^2}\,\mathrm{Re}\left\{\sum_{i=1}^{4}(-1)^{i-1}\mathrm{F}\,(X_i)\right\} \tag{14}$$

for $m \neq n$ and

$$L_{nn}^{(\mathrm{bulk,\,asy})^{(0)}} = \frac{C_\infty}{4\pi\epsilon_n^2\omega^2 s_{\max}^2}\Big(1 - \mathrm{Re}\big\{\mathrm{F}\,(X_0)\big\}\Big) \tag{15}$$

for the diagonal terms; $C_\infty = \lim_{s\to\infty}(|s|(\Gamma(s) - \Gamma^{(\mathrm{el})}(s) - \Gamma^{(\mathrm{saw})}(s)))$, $s_{\max}$ is the slowness value beyond which the Green's function has reached its asymptotic behavior and X_i have the same expressions as in (12) with s_{saw} substituted by $s_{\max}$. Besides, we have introduced the function

$$\mathrm{F}(u) = \mathrm{e}^{-ju} - ju\,\mathrm{e}^{-ju} - u^2\,\mathrm{Expint}(ju) \tag{16}$$

where Expint denotes the exponential integral [11]. By analytically differentiating the previous equations, we obtain the following expressions for $L_{mn}^{(\mathrm{bulk,\,asy})^{(k)}}$ for $k \geq 1$:

$$L_{mn}^{(\mathrm{bulk,\,asy})^{(k)}} = \frac{C_\infty}{4\pi\epsilon_m\epsilon_n s_{\max}^2\omega^{k+2}} \cdot \mathrm{Re}\left\{\sum_{i=1}^{4}(-1)^{(i-1)}\mathrm{R}_k(X_i)\mathrm{e}^{-jX_i}\right\} \tag{17}$$

for $m \neq n$ and

$$L_{nn}^{(\mathrm{bulk,\,res})^{(k)}} = \frac{C_\infty}{2\pi\epsilon_n^2 s_{\max}^2\omega^{k+2}}\left(\chi_k + \mathrm{Re}\{\mathrm{S}_k(X_0)\,\mathrm{e}^{-jX_0}\}\right) \tag{18}$$

for the diagonal terms, where the polynomials R_k and S_k and the coefficient χ_k are easily evaluated from (14) and (15).

The moments $L_{mn}^{(\mathrm{bulk,\,res})^{(k)}}$ are to be computed numerically and, in order to speed up their calculation, we compute in advance and tabulate on a suitable range the frequency-independent functions

$$\Gamma^{(\mathrm{bulk,\,res})^{(k)}}(X) = \frac{1}{2\pi}\int_{-\infty}^{+\infty}(-js)^k\Gamma^{(\mathrm{bulk,\,res})}(s)\,\mathrm{e}^{-jsX}\,\mathrm{d}s. \tag{19}$$

The integration is performed via an adaptive Gauss–Legendre quadrature rule. Inserting $\Gamma^{(\mathrm{bulk,\,res})^{(k)}}(X)$ in (6) and interchanging the order of integration yields

$$L_{mn}^{(\mathrm{bulk,\,res})^{(k)}} = \int_{-\infty}^{+\infty} x^k\Gamma^{(\mathrm{bulk,\,res})^{(k)}}(\omega x)\mathrm{T}_{mn}(x)\,\mathrm{d}x \tag{20}$$

where the subdomain functions

$$\mathrm{T}_{mn}(x) = \frac{1}{4\epsilon_m\epsilon_n}\int_{-\infty}^{+\infty}\mathrm{P}_{W_m}(x-x')\mathrm{P}_{W_n}(x')\,\mathrm{d}x' \tag{21}$$

are evaluated analytically. Also, the integrals defined in (20) are efficiently computed by a Gauss–Legendre quadrature rule based on, typically, $N_{\mathrm{G}} = 10 \div 20$ abscissas.

III. Reduced-Order Model

Recently, different moment-matching techniques have been developed for the efficient analysis of circuits and electromagnetic devices [14], [15], such as the AWE method [16] and Cauchy method [18]. In the AWE method, the response of the system under analysis, i.e., $H(\omega)$, is approximated by its truncated Taylor expansion

$$H(\omega) \cong \hat{H}(\omega) = m_0 + m_1\omega + \cdots + m_{2q-1}\omega^{2q-1} \tag{22}$$

where m_k are the computed $2q$ low-order moments of $H(\omega)$. Since the Taylor expansion has a limited bandwidth, approximation (22) is converted into a Padé rational function, which has a larger domain

$$\hat{H}(\omega) = \frac{b_{q-1}\omega^{q-1} + \cdots + b_1\omega + b_0}{a_q\omega^q + \cdots + a_1\omega + 1}. \tag{23}$$

Setting (22) equal to (23) and cross-multiplying by the denominator yields a set of linear equations that can be solved for the coefficients $\{a_m\}$ and $\{b_m\}$. In the case where one expansion point is not sufficient to cover the desired frequency band, multiple expansion points can be used in order to generate a set of Padé functions [17]. The Cauchy method deals with approximating the response of a system, over the entire band of interest, by a ratio of two polynomials [18]. Given the values of the function and its derivatives at a few points, the coefficients are obtained by solving a linear system by the least square method, whereas the order of the polynomials are estimated via the SVD [19]. It has to be remarked that, in the Cauchy method, the approximation of the system response is accomplished by using the information available in more that one frequency point.

In this paper, we investigate the suitability of the Cauchy method for approximating the frequency response of SAW IDTs, i.e., the transducer input admittance $Y(\omega)$.

A. Cauchy Method

The basic idea of the Cauchy method is to approximate the IDT response $Y(\omega)$ in the frequency range of interest by a the ratio of two polynomials

$$\hat{Y}(\omega) = \frac{A_S(\omega)}{B_D(\omega)} = \frac{\sum_{p=0}^{S}a_p\omega^p}{\sum_{p=0}^{D}b_p\omega^p}. \tag{24}$$

The unknown coefficients a_p and b_p are obtained by equating the estimated moments $\hat{Y}^{(k)}(\omega_j)$ to the known moments $Y^{(k)}(\omega_j)$ [kth angular frequency derivative of $Y(\omega)$ evaluated in the expansion point ω_j with $j = 1 \cdots P$]. This procedure leads to the solution of the linear system

$$[\mathbf{A} \quad -\mathbf{B}]\begin{bmatrix}\mathbf{a}\\ \mathbf{b}\end{bmatrix} = \mathbf{0}. \tag{25}$$

The matrices $\mathbf{A}$ and $\mathbf{B}$ have size $N_{\mathrm{mom}} \times (S+1)$ and $N_{\mathrm{mom}} \times (D+1)$, respectively, where $N_{\mathrm{mom}} = \sum_{j=1}^{P}(N_{\mathrm{mom}}^{(j)} + 1)$ and $N_{\mathrm{mom}}^{(j)}$ is the number of derivatives used in the jth expansion point, and their expressions can be found in [18]. The system (25) is solved by the least-squares method.

A crucial point in the Cauchy method is the evaluation of the degrees S and D. A preliminary choice can be done on the basis of the uniqueness condition for the approximation, i.e., $N_{\mathrm{mom}} \geq S + D + 1$, [18]. Once the matrix $\mathbf{C} = [\mathbf{A} \quad -\mathbf{B}]$ has been computed, the choice of the degrees can be refined by imposing that $S+D+1$ equals the rank of $\mathbf{C}$. A second relation between S and D is obtained by observing that, normally, the choice $D = S + 1$ yields the best approximation [14].

The application of the Cauchy method to the IDT analysis requires the computation of the moments $Y^{(k)}(\omega_j)$. It is easily demonstrated that $Y^{(k)}(\omega)$ can be written as

$$\frac{\mathrm{d}^k Y(\omega)}{\mathrm{d}\omega^k} = \frac{2}{|V|^2}\left\{-\frac{jk}{2}\,\mathbf{\Phi}^T\,\frac{\mathrm{d}^{k-1}\alpha^*(\omega)}{\mathrm{d}\omega^{k-1}} - \frac{j}{2}\,\omega\mathbf{\Phi}^T\,\frac{\mathrm{d}^k\alpha^*(\omega)}{\mathrm{d}\omega^k}\right\} \tag{26}$$

where the derivative of the vector of the charge coefficients is

$$\frac{\mathrm{d}^k\alpha}{\mathrm{d}\omega^k} = \alpha^{(k)} = -\mathbf{L}^{-1}\sum_{i=0}^{k-1} C_{ki}\mathbf{L}^{(k-i)}\alpha^{(i)} \tag{27}$$

with $C_{ki} = k!/[i!(k-i)!]$. Since in the computation of the moments $Y^{(k)}(\omega_j)$ we need to evaluate in each expansion point the inverse of the high rank system matrix $\mathbf{L}$, the numerical efficiency of the method is partly limited. Therefore, in order to keep the algorithm efficient, we generate numerically, as described in Section III-B, a new set of problem-matched basis functions whereby the size of the matrix $\mathbf{L}$ is remarkably reduced.

A practical aspect of the Cauchy method concerns the well-known problem that the explicit use of the moments $Y^{(k)}(\omega_j)$ may result in ill-conditioned numerical computations [14], [17]. A remedy to this problem is to use scaling, i.e., the original moments $Y^{(k)}(\omega_j)$ are replaced by $\eta^k Y^{(k)}(\omega_j)$, where η is a suitable scaling factor. A good choice is the following:

$$\eta = \frac{1}{P}\sum_{j=1}^{P}\left(\frac{|Y^{(0)}(\omega_j)|}{|Y^{(N_{\mathrm{mom}}^{(j)})}(\omega_j)|}\right)^{1./(N_{\mathrm{mom}}^{(j)})}. \tag{28}$$

Although scaling provides better conditioned computations, we observed that the best results are obtained by using moments of order not larger than three or four. Furthermore, in place of using a single approximation in the whole frequency range of interest, it is more convenient to apply different representations of lower order, each defined in a frequency subdomain.

B. Problem-Matched Basis Functions

The numerical efficiency of the Cauchy method described above is related to the size of the system matrix $\mathbf{L}$. This matrix can be small if a set of basis functions is available that fits so closely the actual charge distribution that a small number of them is sufficient for an accurate solution. The task of constructing analytically such a set is very complicated and the evaluation of the matrix elements can be very time consuming. For this reason, we adopted the numerical approach described in [12]. Let $\{\sigma_p^{(\omega)}(x)\}$ with $p = 1, \ldots, P$ be the charge distributions at the P expansion frequencies used in the Cauchy method. They are obtained by the GFM, as described in Section II, and have the following representation in the pulse function basis $\{f_n(x)\}$:

$$\sigma_p^{(\omega)}(x) = \sum_{n=1}^{N} A_{np} f_n(x) \tag{29}$$

where $A_{np} = \alpha_n(\omega_p)$ with $n = 1, \ldots, N$ and $p = 1, \ldots, P$. If these P charge distributions are used as basis functions, they are certainly problem matched. However, they are generally far from being orthogonal and this has adverse consequences in the application of the Cauchy method, which is known to be an ill-conditioned algorithm. This problem can be solved by applying the SVD to the $N \times P$ matrix $\mathbf{A}$ with elements A_{np} introduced in (29). This decomposition has the form $\mathbf{A} = \mathbf{USV}^{\mathrm{H}}$, where $\mathbf{U}$ is a $N \times N$ unitary matrix, $\mathbf{S}$ is a $N \times P$ diagonal matrix with positive elements (singular values), and $\mathbf{V}$ is a $P \times P$ unitary matrix [13]. The columns of $\mathbf{U}$ are the singular vectors $\{\mathbf{u}_{\mathrm{p}}\}$ and those corresponding to nonzero singular values $\{S_p\}$ form an orthonormal basis in the subspace spanned by the charge vectors $\boldsymbol{\alpha}(\omega_p)$. The significance of the various singular vectors $\{\mathbf{u}_{\mathrm{p}}\}$ in the description is measured by the amplitude of the corresponding singular values S_p. Since they range over several orders of magnitude, not all the singular vectors are needed to obtain accurate results in the response curve. Also, inspection of the dynamic range of the singular value set allows us to ascertain whether the frequency sampling is adequate. A small range means, in fact, that the corresponding singular vectors do not have sufficient span for an acceptable representation of the charge distribution. Let $Q \leq P$ be the number of singular vectors assumed to be adequate to represent the charge distribution. Hence, Q is the "effective dimension" of the subspace that contains the charge representation, at least in the band of interest. Define a new set of basis functions via

$$g_l(x) = \sum_{n=1}^{N} f_n(x)u_{nl}, \qquad l = 1, \ldots, Q \tag{30}$$

which can be interpreted as a set of "orthogonalized problem-matched basis functions." They lead to the definition of a new moment matrix

$$\mathbf{K} = \mathbf{U}_Q^{\mathrm{H}}\mathbf{L}\mathbf{U}_Q \tag{31}$$

where the $N \times Q$ matrix $\mathbf{U}_Q$ consists of the first Q columns of the matrix $\mathbf{U}$. In the basis defined by (30), the moments $Y^{(k)}(\omega)$ can be written as

$$\frac{\mathrm{d}^k Y(\omega)}{\mathrm{d}\omega^k} = \frac{2}{|V|^2}\left\{-\frac{jk}{2}\,\mathbf{\Phi}^T\mathbf{U}_Q^*\,\frac{\mathrm{d}^{k-1}\theta^*(\omega)}{\mathrm{d}\omega^{k-1}} - \frac{j}{2}\,\omega\mathbf{\Phi}^T\mathbf{U}_Q^*\frac{\mathrm{d}^k\theta^*(\omega)}{\mathrm{d}\omega^k}\right\} \tag{32}$$

where

$$\frac{\mathrm{d}^k\theta}{\mathrm{d}\omega^k} = \theta^{(k)} = -\mathbf{K}^{-1}\sum_{i=0}^{k-1} C_{ki}\mathbf{K}^{(k-i)}\theta^{(i)} \tag{33}$$

and θ is the vector of the charge coefficients in the new basis. Therefore, the present implementation of the Cauchy method is very efficient because the derivatives of $\mathbf{K}$ are computed analytically as explained in the previous sections and the size of $\mathbf{K}$ is much smaller than that of $\mathbf{L}$.

C. Summary of the Numerical Procedure

In this subsection, we summarize the numerical procedure for the evaluation of the approximated input admittance $\hat{Y}(\omega)$ based on the reduced-order model. The main steps are as follows.

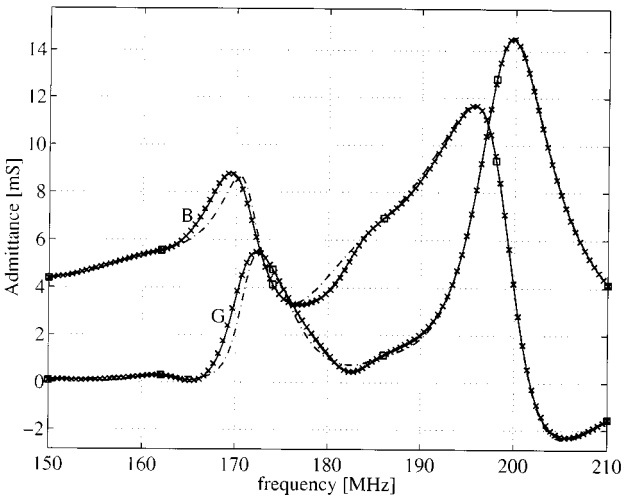

Fig. 2. Input admittance of a 40-finger uniform IDT. Standard GFM (×), reduced-order model with $N_{\rm mom}^{(j)} = 1$ (–·–), reduced-order model with $N_{\rm mom}^{(j)} = 2$ (–), both based on six expansion points (□).

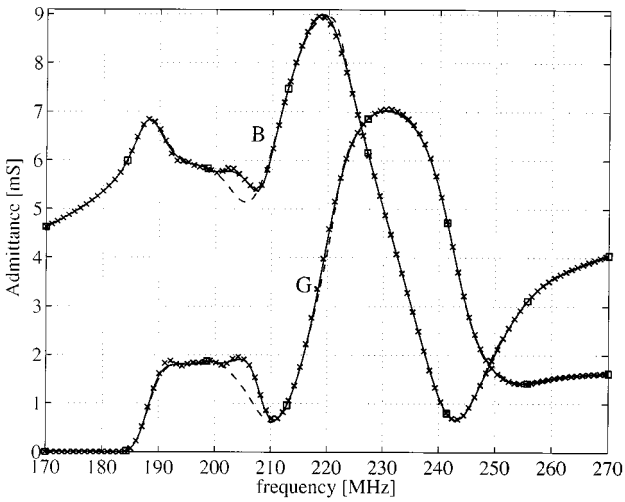

Fig. 3. Input admittance of the apodized IDT described in the text. Standard GFM (×), reduced-order model with $N_{\rm mom}^{(j)} = 2$ (– –), reduced-order model with $N_{\rm mom}^{(j)} = 3$ (–), both based on eight expansion points (□).

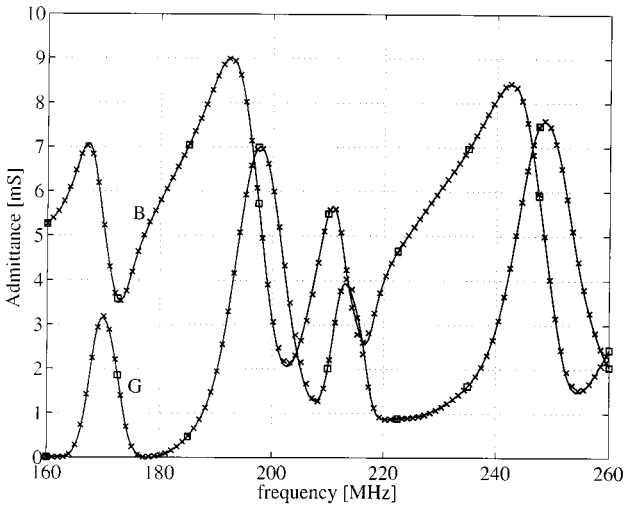

Fig. 4. Input admittance of the apodized IDT described in the text. Standard GFM (×), reduced-order model with $N_{\rm mom}^{(j)} = 3$ (–) and based on nine expansion points (□).

Step 1) Evaluate the charge coefficients vectors α's at each of the P selected frequency points via the standard GFM.

Step 2) Compute the SVD of matrix $\mathbf{A}$, (29), and inspect the dynamic range of the singular values. If the span is not sufficient, then, add a frequency point and repeat Step 1). Otherwise, select the Q most significant singular vectors and define the projection matrix $\mathbf{U}_Q$.

Step 3) For each expansion point ω_p, define the new system matrix $\mathbf{K}$ and compute the moments $Y^{(k)}(\omega_p)$ via (32) and (33).

Step 4) For each frequency subdomain, typically containing two/three expansion points, set $D = S + 1$ and $S + D = N_{\rm mom} - 1$ and build matrix $\mathbf{C} = [\mathbf{A} \quad -\mathbf{B}]$, (25). On the basis of the SVD of matrix $\mathbf{C}$, redefine the choice of the polynomials degrees so that $\rho(C) = S + D + 1$. Solve the linear system (25) via the least-square method and evaluate the input admittance over the entire frequency subdomain.

IV. Numerical and Experimental Results

We applied the present method to the analysis of IDTs for integrated acoustooptic devices in X–Y $LiNbO_3$ operating at optical wavelengths around $\lambda \cong 1.55$ μm. In these devices, the IDTs are designed in order to exhibit a SAW resonance at about 172 MHz [20]. In all the results based on the reduced-order model, we used different approximations in each frequency subdomain defined between two expansion points. As an example of the accuracy of the reduced-order model, Fig. 2 shows the input admittance of a uniform IDT with 40 fingers. In this figure, we compare the simulation performed via the standard GFM with four basis functions per finger, the simulation obtained by the reduced-order model with $N_{\rm mom}^{(j)} = 1$ and $N_{\rm mom}^{(j)} = 2$ derivatives per expansion point. In the application of the SVD method, the ratio of the smallest to the largest singular value is 0.02 and all the singular vectors have been used as new basis ($Q = P$). The resonance at the lower frequency is related to the generation of a SAW, while the one at 198 MHz is associated to the excitation of bulk waves with quasi-shear horizontal (QSH) polarization. The reduced-order model with $N_{\rm mom}^{(j)} = 1$ is already in good agreement with the GFM solution, but the introduction of the second derivatives in the model enables to reduce the difference to negligible values. The CPU time is practically the same in the two cases and about one order of magnitude smaller than that of the standard GFM.

In order to further validate the model, we also consider apodized transducers. Figs. 3 and 4 show the input admittance of two different apodized IDTs with dummy fingers and with a fundamental cell containing three electrodes, with voltages $+V_0$, $+V_0$, and $-V_0$. The first transducer exhibits a -3-dB band of about 20 MHz centered around $f = 198$ MHz, while the second IDT was designed to exhibit a SAW resonance at both 172 and 210 MHz. In both cases, the reduced-order model with $N_{\rm mom}^{(j)} = 3$ yields results that are indistinguishable from those obtained via the direct application of the GFM,

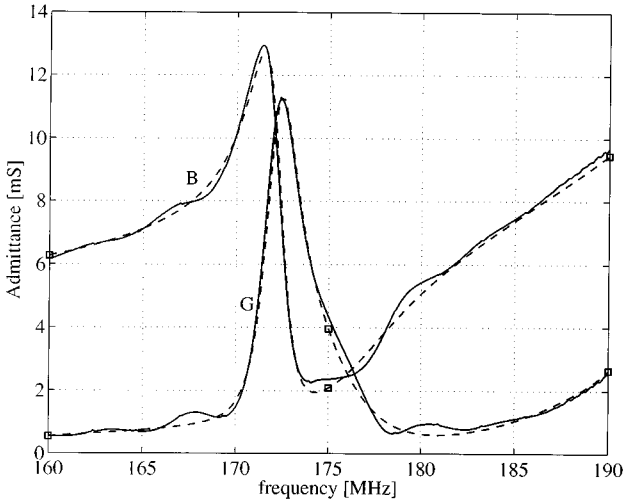

Fig. 5. Input admittance of an 80-finger uniform IDT. Measurement (—), reduced-order model with $N_{\mathrm{mom}}^{(j)} = 3$ (– –) and based on three expansion points (□).

but enables to remarkably speed up the evaluation of the IDT frequency response. Moreover, in both cases, $Q = P$ was taken and the ratios of the smallest to the largest singular value are 0.0092 and 0.0089, respectively.

As a last example of validity of the present technique, in Fig. 5, we plotted the simulated and measured input admittance of a uniform IDT with 80 fingers. The simulation was performed by the reduced-order model with six basis functions per finger, $P = 3$ expansion points, and $N_{\mathrm{mom}}^{(j)} = 3$ derivatives in each expansion point, and was corrected for the value of the parasitic capacitance C_{p} (mostly due to the bonding pads) and the metallization loss resistance R_{Ω}. We may observe that the information included in the model enables to accurately predict the SAW resonance at about 172 MHz, neglecting only small details that are associated to highest derivatives of the frequency response. Moreover, the required CPU time is more than one order of magnitude smaller in comparison with the direct application of the GFM, implemented with the GMRES algorithm for the solution of the linear system.

V. Conclusions

In this paper, we have presented a novel model order-reduction technique for the rigorous analysis of SAW IDTs. Numerical and experimental results confirm the efficiency and accuracy of the method. Since the present technique has been successfully applied to a two-dimensional analysis in which the mass-loading effect is neglected, we are planning to investigate the suitability of the method to be extended to the three-dimensional analysis based on the complete 4×4 dyadic Green's function, where the CPU time reduction should be even more impressive.

References

[1] P. Ventura, J. M. Hodé, M. Solal, J. Desbois, and J. Ribbe, "Numerical methods for SAW propagation characterization," in *Proc. IEEE Ultrason. Symp.*, 1998, pp. 175–186.

[2] R. C. Peach, "Green function analysis for SAW devices with arbitrary electrode structures," in *Proc. IEEE Ultrason. Symp.*, 1997, pp. 99–103.

[3] P. Ventura, J. M. Hodé, and B. Lopes, "Rigorous analysis of finite SAW devices with arbitrary electrode geometries," in *Proc. IEEE Ultrason. Symp.*, 1995, pp. 257–262.

[4] O. Männer, K. C. Wagner, and C. C. W. Ruppel, "Advanced numerical methods for the simulation of SAW devices," in *Proc. IEEE Ultrason. Symp.*, 1996, pp. 123–130.

[5] J. E. Bracken and Z. J. Cendes, "Asymptotic waveform evaluation for S-domain solution of electromagnetic devices," *IEEE Trans. Magn.*, vol. 34, pp. 3232–3235, Sept. 1998.

[6] K. Lim Choi and M. Swaminathan, "Utilization of fast algorithm to Analyze embedded passive components using commercial EM Solvers," in *6th IEEE Elect. Performance Electron. Packag. Topical Meeting*, 1997, pp. 240–243.

[7] R. F. Milsom, "Bulk wave generation by the IDT," in *Computer-Aided Design of Surface Acoustic Wave Devices*. Amsterdam, The Netherlands: Elsevier, 1976, pp. 64–81.

[8] O. A. Peverini, R. Orta, and R. Tascone, "Rigorous electromechanical analysis of X–Y $LiNbO_3$ interdigital transducers," in *Proc. ICEAA99*, pp. 145–148.

[9] R. F. Milsom, N. H. Reilly, and M. Redwood, "Analysis of generation and detection of surface and bulk acoustic waves by interdigital transducers," *IEEE Trans. Sonics Ultrason.*, vol. SU-24, pp. 147–166, May 1977.

[10] A. R. Baghai-Wadji, O. Männer, and R. Ganß-Puchstein, "Analysis and measurement of transducer end radiation in SAW filters on strongly coupling substrates," *IEEE Trans. Microwave Theory Tech.*, vol. 37, pp. 150–158, Jan. 1989.

[11] M. Abramowitz and I. A. Stegun, *Handbook of Mathematical Functions*. New York: Dover, 1970, pp. 228–254.

[12] C. K. Aanandan, P. Debernardi, R. Orta, R. Tascone, and D. Trinchero, "Problem-matched basis functions for moment method analysis—An application to reflection gratings," *IEEE Trans. Antennas Propagat.*, vol. 48, pp. 35–40, Jan. 2000.

[13] G. H. Golub and C. F. Van Loan, *Matrix Computations*. Baltimore, MD: The Johns Hopkins Univ. Press, 1983, ch. 2–3.

[14] P. Feldmann and R. Freund, "Efficient linear circuit analysis by Padé approximation via the Lanczos process," *IEEE Trans. Computer-Aided Design*, vol. 14, pp. 639–649, May 1995.

[15] J. Gong and J. L. Volakis, "AWE implementation for electromagnetic FEM analysis," *Electron. Lett.*, vol. 32, no. 24, pp. 2216–2217, 1996.

[16] X. Zhang and J. Lee, "Application of the AWE method with the 3-D TVFEM to model spectral responses of passive microwave components," *IEEE Trans. Microwave Theory Tech.*, vol. 46, pp. 1735–1741, Nov. 1998.

[17] E. Chiprout and M. S. Nakhla, *Asymptotic Waveform Evaluation and Moment Matching for Interconnect Analysis*. Norwell, MA: Kluwer, 1994.

[18] K. Kottapalli, T. K. Sarkar, Y. Hua, E. K. Miller, and G. J. Burke, "Accurate computation of wide-band response of electromagnetic systems utilizing narrow-band information," *IEEE Trans. Microwave Theory Tech.*, vol. 39, pp. 682–687, Apr. 1991.

[19] R. S. Adve, T. K. Sarkar, S. M. Rao, E. K. Miller, and D. R. Pflug, "Application of the Cauchy method for extrapolating/interpolating narrow-band system responses," *IEEE Trans. Microwave Theory Tech.*, vol. 45, pp. 837–845, May 1997.

[20] C. Duchet, C. Brot, and M. Di Maggio, "Interdigital transducer for acousto-optic tunable filter on $LiNbO_3$," *Electron. Lett.*, vol. 31, no. 15, pp. 1235–1237, 1995.

Oscar Antonio Peverini was born in Lisbon, Portugal, in 1972. He received the Laurea degree in telecommunications engineering (*summa cum laudae*) at the Politecnico di Torino, Turin, Italy, in 1997, and is currently working toward the Ph.D. degree in electronic engineering at the Politecnico di Torino.

From August 1999 to March 2000, he was a Visiting Member at the Applied Physics/Integrated Optics Department, University of Paderborn, Paderborn, Germany. His research interests include numerical simulation and design of SAW waveguides and IDTs for integrated acoustooptical devices.

Renato Orta (M'92–SM'99) received the Laurea degree in electronic engineering from the Politecnico di Torino, Turin, Italy, in 1974.

Since 1974, he has been a member of the Department of Electronics, Politecnico di Torino, first as Assistant Professor, then as Associate Professor and, since 1999, as Full Professor. In 1985, he was a Research Fellow at the European Space Research and Technology Center (ESTEC) European Space Agency (ESA), Noordwijk, The Netherlands. In 1998, he was a Visiting Professor (CLUSTER Chair) at the Technical University of Eindhoven, Eindhoven, The Netherlands. He currently teaches courses on electromagnetic field theory and optical components. His research interests include the areas of microwave and optical components, radiation and scattering of electromagnetic and elastic waves, and numerical techniques.

Riccardo Tascone was born in Genoa, Italy, in 1955. He received the Laurea degree in electronic engineering from the Politecnico di Torino, Turin, Italy, in 1980.

From 1980 to 1982, he was with the Centro Studi e Laboratori Telecomunicazioni (CSELT), Turin, Italy, where his research mainly dealt with frequency-selective surfaces, waveguide discontinuities, and microwave antennas. In 1982, he joined the Centro Studi Propagatione e Antenne (CESPA), Consiglio Nazionale delle Ricerche (CNR), Turin, Italy, where he was initially a Researcher and, since 1991, a Senior Scientist (Dirigente di Ricerca). He is currently Head of the Applied Electromagnetics Section, Istituto di Ricerca sull'Ingeneria delle Telecomunicazioni e dell'Informazione (IRITI), a newly established institute of the CNR. He has held various teaching positions in the area of electromagnetics at the Politecnico di Torino. His current research activities are in the areas of microwave antennas, dielectric radomes, frequency-selective surfaces, radar cross section, waveguide discontinuities, microwave filters, multiplexers, and optical passive devices.